Chapter 10
Ab Initio Path Integral Molecular Dynamics Simulations of F_2H^- and $F_2H_3^+$

K. Suzuki, H. Ishibashi, K. Yagi, M. Shiga, and M. Tachikawa

Abstract The quantum nature of the strong hydrogen bonds for the F_2H^- and $F_2H_3^+$ ions and their deuterated isotopomers at the room temperature has been studied using ab initio path integral molecular dynamics (PIMD) simulations. It is found that, for both of these ions, the hydrogen-bonded H/D atoms largely fluctuate around the central position of two F atoms. The average FH/FF distances of F_2H^- and $F_2H_3^+$ are longer than the average FD/FF distances of F_2D^- and $F_2D_3^+$ due to the primary/secondary isotope effects, which stem from the difference of the quantum nature of H and D nuclei. These results are compared with the family of Zundel-type ions, $O_2H_3^-$, $N_2H_5^-$, $O_2H_5^+$, and $N_2H_7^+$, which have been studied previously with the same ab initio PIMD approach. A comparison is also made with the previous experimental and ab initio vibrational configuration interaction results of F_2H^-.

K. Suzuki · H. Ishibashi · M. Tachikawa (✉)
Quantum Chemistry Division, Graduate School of Science, Yokohama-city University, Seto 22-2, Kanazawa-ku, Yokohama, 236-0027, Japan,
e-mail: v065302@yokohama-cu.ac.jp; tachi@yokohama-cu.ac.jp

K. Yagi
Department of Chemistry, University of Illinois at Urbana-Champaign, 600 South Mathews Avenue, Urbana, IL, 61801, USA,
e-mail: kyagi@illinois.edu

M. Shiga
CCSE, Japan Atomic Energy Agency (JAEA), Kashiwanoha 5-1-5, Kashiwa, Chiba, 277-8587, Japan,
e-mail: shiga.motoyuki@jaea.go.jp

K. Nishikawa et al. (eds.), *Quantum Systems in Chemistry and Physics*,
Progress in Theoretical Chemistry and Physics 26, DOI 10.1007/978-94-007-5297-9_10,

10.1 Introduction

Hydrogen is inherently quantum mechanical due to its small mass, and the basic understanding of hydrogen bonding, which is ubiquitous in nature, should be rooted in quantum mechanics and quantum statistics. In most cases, the bonded proton belongs to a molecule weakly interacting with other molecules. However, in some strongly hydrogen-bonded systems, which are usually found to be in an ionic form, the proton is shared by the two molecular moieties forming low-barrier hydrogen bonds or symmetric hydrogen bonds [1–4]. One representative example is the Zundel cation of protonated water dimer, $O_2H_5^+$ [5–7], and its isoelectronic species, such as $F_2H_3^+$ [8, 9] and $N_2H_7^+$ [10–12], as well as the anionic variations, F_2H^-[13–22], $O_2H_3^-$ [5, 6, 23–26], and $N_2H_5^-$ [11]. Here, we focus on the F_2H^- and $F_2H_3^+$ ions, which possess strong hydrogen bonds among this family of Zundel-type ions. The bifluoride anion, F_2H^-, has been detected experimentally [13–16] and is well-known to have the symmetric hydrogen bond from the vibrational spectrum as well as ab initio electronic structure calculations [17–22]. The spectroscopic characterization of the F_2H^- ion has been a challenging issue for its strong anharmonic nature. Hirata et al. [21] have recently clarified the assignment of vibrational spectra using vibrational configuration interaction (VCI) calculation on a high-quality Born–Oppenheimer (BO) potential energy surface [27]. There, it has been shown that the anharmonicity and mode coupling are indispensable to understand the vibrational structure of F_2H^- ion. For the $F_2H_3^+$ cation, meanwhile, ab initio electronic structure calculations have reported that its equilibrium structure has a symmetric hydrogen bond [8, 9]. However, the effect of molecular vibration must be taken into account to be more quantitative. In this chapter, we report ab initio path integral molecular dynamics (PIMD) simulations of the F_2H^- and $F_2H_3^+$ ions and their deuterated isotopomers to study the quantum nature of these strong hydrogen-bonded species at 300 K. The ab initio PIMD is a first-principles approach, which is capable of providing insights into complex many-body effects in hydrogen bonds [3–6, 11, 25, 26, 28–34]. In this simulation, the nuclear quantum effect is fully taken into account for all the vibrational degrees of freedom. Here, the important approximation is the BO surface evaluated $on\ the\ fly$ during the simulation which is designated by the quality of the electronic structure theory (i.e. in the present case, the second-order Møller – Plesset perturbation theory (MP2) and 6-31++G** basis set) and the number of imaginary time slices in Suzuki–Trotter expansion (i.e., the number of beads, $P = 16$ in this study). The results are compared with those of the conventional ab initio molecular dynamics (MD) simulations in which the nuclei are treated as classical particles in order to clarify the role of nuclear quantum effect in these systems.

10.2 Computational Details

The ab initio MD and ab initio PIMD simulations have been carried out in a similar way as in the previous works [6, 11, 25, 26, 31–33] using our program code [35]. The code implements the MD and PIMD routines, which runs in conjunction with Gaussian 03 program package [36]. The BO energy and forces are calculated *on the fly* at the MP2/6-31++G** level of ab initio theory. We have employed massive Nosé – Hoover thermostat [37, 38] with the chain length $L = 4$ using normal mode transformation [39] to strongly control the system temperature at 300 K. Ab initio PIMD simulations of F_2H^-(F_2D^-) and $F_2H_3^+$ ($F_2D_3^+$) with $P = 16$ beads have been run for 50,000 steps and 150,000 steps after a thermal equilibration of 5,000 steps, respectively, using a time step size $\Delta t = 0.1$ fs ($\Delta t = 0.15$ fs). Ab initio MD simulations of F_2H^- and $F_2H_3^+$ (corresponding to $P = 1$ condition) have been run for 200,000 steps and 500,000 steps after a thermal equilibration of 5,000 steps, respectively, with the time step size $\Delta t = 0.1$ fs. Note that the simulations of $F_2H_3^+$ were run longer than those of F_2H^- since more statistics should be gained with respect to the configurations of non-bonded protons. The statistical errors of average bond lengths and bond angles have been estimated by the block average method [40].

10.3 Results and Discussion

10.3.1 Static Calculations

Before starting the simulation, we have checked the quality of MP2/6-31++G** method for F_2H^- (Fig. 10.1a) and $F_2H_3^+$ (Fig. 10.1b) in terms of the conventional static ab initio calculations. The interatomic distance and the bond angle are

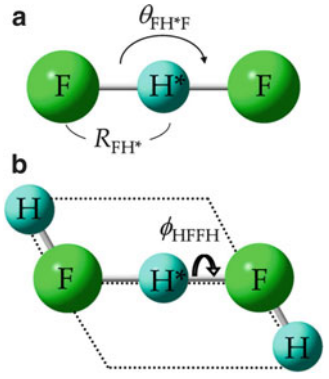

Fig. 10.1 Schematic illustration of the equilibrium structures of (**a**) F_2H^- and (**b**) $F_2H_3^+$

Table 10.1 Interatomic distances R_{FH^*}, R_{FF} (in Å), bond angle θ_{FH^*F} (in degrees), and barrier height ΔE (in kcal/mol) obtained from static ab initio calculations of F_2H^- and $F_2H_3^+$ using 6-31++G** basis set

	F_2H^-	$F_2H_3^+$				
		Equilibrium	Transition state			
	R_{FH^*}	R_{FH^*}	R_{FH^*}	R_{FF}	θ_{FH^*F}	ΔE
HF	1.125	1.132	1.133	2.259	170	1.60
B3LYP	1.151	1.155	1.156	2.300	168	1.52
MP2	1.149	1.151	1.152	2.293	168	1.61
CCSD	1.143	1.147	1.148	2.286	169	1.63
CCSD(T)	1.146	1.148	1.149	2.288	169	1.63

defined in Fig. 10.1, where the proton (deuteron) in the hydrogen bond is labeled as H^* (D^*). The equilibrium structures of the F_2H^- and $F_2H_3^+$ ions have the $D_{\infty h}$ and C_{2h} symmetries, respectively, where the protons are located at the center of two fluorine atoms. The $F_2H_3^+$ ion has a trans-conformation with $=180°$, while the cis-conformation with $=0°$ is a transition state with the barrier height of $\Delta E = 1.6$ kcal/mol from the equilibrium structure. This transition state has the C_{2v} symmetry wherein the θ_{FH^*F} angle is bent from 180° to a small extent. In Table 10.1, we list the equilibrium geometries obtained at the MP2/6-31++G** level, as well as those at the level of Hartree–Fock theory (HF), density functional theory with B3LYP exchange correlation functional, coupled-cluster singles and doubles (CCSD), and CCSD with non-iterative triples correction (CCSD(T)) using the same 6-31++G** basis set. For both F_2H^- and $F_2H_3^+$ ions, the HF method estimates the FF distance slightly shorter than the most accurate CCSD(T), while B3LYP, MP2, and CCSD results are closer to the CCSD(T) result. However, it is found that the barrier height ΔE is underestimated in B3LYP, while the result of MP2 reasonably agrees with that of CCSD and CCSD(T). In the comparison of F_2H^- between this work and previous result by Hirata et al. [21], the result of 6-31++G** basis set is slightly underestimated in CCSD/aug-cc-pCVTZ level (1.136 Å). Thus, the present method (MP2/6-31++G**) overestimates though not very seriously. As the MP2/6-31++G** level should be sufficient for our purpose to study the nuclear quantum effect with reasonable accuracy and efficiency, we have decided to choose MP2/6-31++G** for the ab initio MD and ab initio PIMD simulations for the systems of current interest.

10.3.2 MD and PIMD Simulations

In Tables 10.2 and 10.3, we list the average distances R_{FH^*}, R_{FF}, and R_{FH} and the average angles θ_{FH^*F}, θ_{HFF}, and ϕ_{HFFH} obtained by ab initio PIMD and ab initio MD simulations for the F_2H^- and $F_2H_3^+$ ions. It is found that the average values of and are systematically larger in the order of the equilibrium values, the average values in the ab initio MD, the average values in the ab initio PIMD of the D-isotopomer, and the ab initio PIMD of the H-isotopomer. It is also found that the average values of and become smaller in the same order. This order exactly corresponds to the extent

Table 10.2 Average values of interatomic distances R_{FH^*}, R_{FF} (in Å), and bond angle θ_{FH^*F} (in degrees) obtained from ab initio MD simulations of F_2H^- and ab initio PIMD simulations of F_2H^- and F_2D^-. The root mean square values of distributions of R_{FH^*}, R_{FF}, and θ_{FH^*F} are given in the parenthesis

	R_{FH^*}			R_{FF}			θ_{FH^*F}		
Ab initio MD, F_2H^-	1.158	±	0.001	2.311	±	0.001	173.4	±	0.6
	(0.065)			(0.044)			(3.6)		
Ab initio PIMD, F_2D^-	1.163	±	0.001	2.324	±	0.001	169.6	±	0.4
	(0.097)			(0.058)			(5.4)		
Ab initio PIMD, F_2H^-	1.165	±	0.001	2.328	±	0.002	166.7	±	0.3
	(0.111)			(0.059)			(6.9)		

Table 10.3 Average values of interatomic distances R_{FH^*}, R_{FF} (in Å), bond angle θ_{FH^*F}, and torsion angle ϕ_{HFFH} (in degrees) obtained from ab initio MD simulations of $F_2H_3^+$ and ab initio PIMD simulations of $F_2H_3^+$ and $F_2D_3^+$. The root mean square values of distributions of R_{FH^*}, R_{FF}, and θ_{FH^*F} are given in the parenthesis

	R_{FH^*}			R_{FF}			R_{FH}		
Ab initio MD, $F_2H_3^+$	1.163	±	0.001	2.311	±	0.001	0.9531	±	0.0001
	(0.067)			(0.051)			(0.0214)		
Ab initio PIMD, $F_2D_3^+$	1.168	±	0.001	2.322	±	0.001	0.9635	±	0.0002
	(0.096)			(0.059)			(0.0570)		
Ab initio PIMD, $F_2H_3^+$	1.173	±	0.001	2.329	±	0.001	0.9680	±	0.0003
	(0.108)			(0.063)			(0.0622)		

	θ_{FH^*F}			θ_{HFF}			ϕ_{HFFH}		
Ab initio MD, $F_2H_3^+$	168.9	±	0.3	120.6	±	0.1	132	±	4
	(5.8)			(9.1)			(36)		
Ab initio PIMD, $F_2D_3^+$	165.3	±	0.4	121.4	±	0.4	126	±	4
	(7.6)			(10.3)			(41)		
Ab initio PIMD, $F_2H_3^+$	163.4	±	0.4	121.5	±	0.5	122	±	8
	(8.5)			(11.3)			(44)		

of vibrational fluctuation due to classical thermal excitation and quantum zero-point motion. To see this more clearly, we display the probability density with respect to the distances and for F_2H^- and $F_2H_3^+$ ions, respectively, in Figs. 10.2 and 10.3. We can see that the width of the distribution becomes broader and the peak position makes a shift to a longer distance in the same order as above. For instance, the peaks are found at (R_{FH^*}, R_{FF}) = (1.15, 2.31 Å) for ab initio MD of F_2H^-, (1.16, 2.32 Å) for ab initio PIMD of F_2D^-, and (1.17 Å, 2.34 Å) for ab initio PIMD of F_2H^-. The same tendency is also found in the case of $F_2H_3^+$. Therefore, it is concluded that, in both cases of F_2H^- and $F_2H_3^+$, the nuclear quantum effect stretches the FH* and FF distances due to the potential anharmonicity. In Figs. 10.2 and 10.3, we have also shown the probability density with respect to the relative position of H*, $\delta_{FH^*} = R_{FH^*} - R_{H^*F}$, to confirm that the H* atom is widely vibrating, but that the distributions are peaked at the center of two fluorine atoms, $\delta_{FH^*} = 0$.

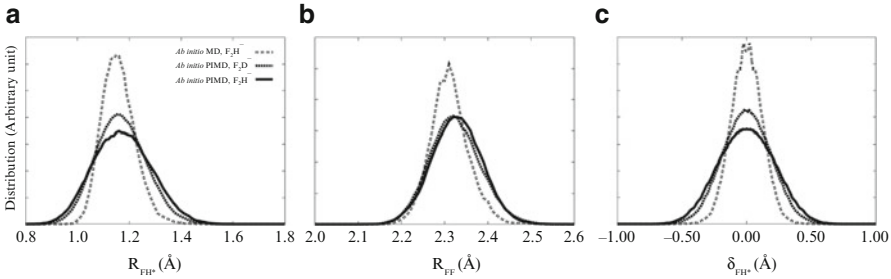

Fig. 10.2 Probability density of F_2H^- with respect to (**a**) R_{FH^*}, (**b**) R_{FF}, and (**c**) δ_{FH^*}

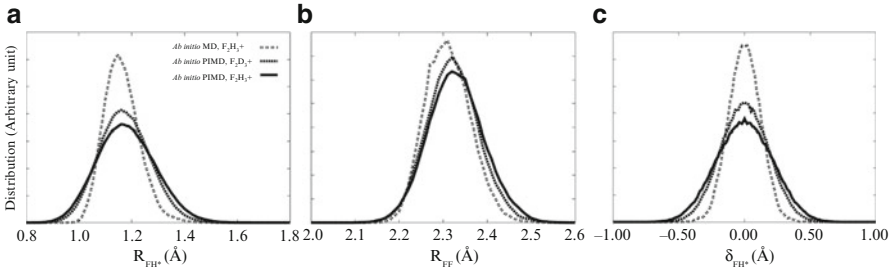

Fig. 10.3 Probability density of $F_2H_3^+$ with respect to (**a**) R_{FH^*}, (**b**) R_{FF}, and (**c**) δ_{FH^*}

By comparing the results of ab initio MD and ab initio PIMD simulations, we find that the average FH* and FF distances are shifted by about 0.007 and 0.017 Å, respectively, for F_2H^- and about 0.005 and 0.013 Å, respectively, for F_2D^-. In the previous study [21], the equilibrium FH* distance has been found to be 1.136 Å while the FH* distance averaged over the zero-point vibrational state obtained from ab initio VCI has been found to be 1.154 Å, and thus, the shift is 0.018 Å. In the present study, the equilibrium FH* distance is 1.149 Å while the average distance in ab initio PIMD simulation at 300 K is 1.165 Å, and thus, the shift is 0.016 Å. It is interesting that the shifts obtained from the two different methods, i.e., PIMD and VCI, are in good agreement. As the FH* vibration has a relatively high frequency, the zero-point vibrational average in VCI and the nuclear quantum effect at the temperature 300 K in PIMD may be effectively similar. Although the absolute value of the FH* distance is affected by the difference in the level of ab initio BO potential energy surfaces employed in these calculations, the shift seems to be relatively insensitive to it. For the same reason as in the case of F_2H^-, the average FH* and FF distances of $F_2H_3^+$ are shifted by about 0.010 and 0.018 Å., respectively, from the equilibrium values, while the average FD* and FF distances of $F_2D_3^+$ are shifted by about 0.005 and 0.011 Å, respectively, from the equilibrium values. The structural shifts upon the isotopic substitution, which is called the geometrical isotope effect

Table 10.4 Equilibrium interatomic distances R_{XH^*}/R_{XD^*}/ and R_{XX} obtained from static ab initio calculation, and average values of interatomic distances R_{XH^*}/R_{XD^*}/ and R_{XX} obtained from ab initio PIMD simulations, where X = F, O, or N. The unit is in Å

		Static	MD	PIMD			Static	MD	PIMD		
X		R_{XH^*}	R_{XH^*}	R_{XD^*}	R_{XH^*}	R_{XH^*}-R_{XD^*}	R_{XX}	R_{XX}	$R_{XX}^{(D)}$	$R_{XX}^{(H)}$	$R_{XX}^{(H)}$-$R_{XX}^{(D)}$
F	F_2H^-	1.149	1.158	1.163	1.165	0.002	2.299	2.311	2.324	2.328	0.004
	$F_2H_3^+$	1.151	1.163	1.168	1.173	0.005	2.302	2.311	2.322	2.329	0.007
O	$O_2H_5^+$ [a]	1.194	–	1.220	1.224	0.004	2.386	–	2.418	2.422	0.004
	$O_2H_3^-$ [a]	1.095/1.398	–	1.262	1.261	−0.001	2.491	–	2.504	2.498	−0.006
N	$N_2H_7^+$ [b]	1.111/1.594	1.369	1.353	1.352	−0.001	2.705	2.727	2.687	2.678	−0.009
	$N_2H_5^-$ [b]	1.053/1.855	1.500	1.508	1.480	−0.028	2.904	2.965	2.972	2.916	−0.056

[a] $O_2H_5^+$ and $O_2H_3^-$ [16]

[b] $N_2H_7^+$ and $N_2H_5^-$ [11]

(GIE), are purely a quantum mechanical effect, which is absent in the framework of classical statistics. In the present case, it is considered that the shifts in the FH* and FD* bond lengths are a direct consequence of GIE, while the shifts in the FF separations are secondary consequences of GIE.

In our previous reports on the Zundel ion $O_2H_5^+$ [6] and its isoelectronic species [11], it has been discussed that the GIE in strong hydrogen bonds may have two competing effects either to shorten hydrogen bonds due to strengthening or to lengthen due to weakening by substituting proton to deuteron. The former GIE is dominant in the cases for $O_2H_5^+$ as well as $O_2H_3^-$ at low temperatures [25], while the latter GIE becomes dominant for $N_2H_7^+$, $N_2H_5^-$ [11], and $O_2H_3^-$ at high temperatures [6, 25]. We summarize the data for this work as well as the previous works in Table 10.4. Here we can see a tendency that the former GIE prevails for systems with short heavy-atom separations, while the latter prevails for systems with long heavy-atom separation. As the F_2H^- and $F_2H_3^+$ ions have strong hydrogen bonds, they belong to the former category. Although the data is limited, the turnover of these effects seems to occur when the heavy-atom separation is about 2.5 Å.

Finally, Fig. 10.4 shows the probability density with respect to the torsion angle obtained from the ab initio MD and ab initio PIMD simulations of the $F_2H_3^+$ ion. Also a two-dimensional distribution with respect to and is shown in the supporting information (S1). The results show that the ion is fluctuating around the trans-conformation (= 180°), but there is also non-negligible distribution at the cis-conformation (= 0°) allowing for a hindered rotation. The distribution at the cis-conformation obtained from ab initio PIMD simulations is slightly larger than that from the ab initio MD simulation. From Fig. S1, H-H bond length in ab initio PIMD simulations tends to be longer as it becomes close to cis-conformation, contrary to ab initio MD simulations. These results suggest that the effective free energy surface of ab initio PIMD simulation is different from that of ab initio MD simulation due to the nuclear quantum effect.

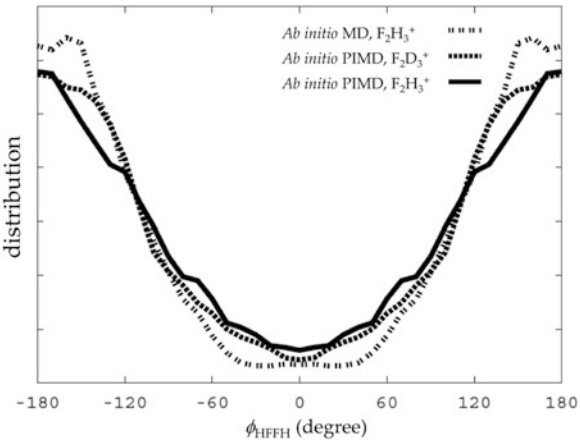

Fig. 10.4 Probability density of $F_2H_3^+$ with respect to ϕ_{HFFH}

10.4 Conclusions

The structures of the F_2H^- and $F_2H_3^+$ ions and their deuterated isotopomers at the room temperature have been studied in detail by ab initio PIMD simulation. For both ions, it is found that the hydrogen-bonded H/D atom is vibrating with large amplitude around the center of two fluorine atoms due to thermal and quantum effects. Large fluctuation is also found for the non bonded hydrogen in the $F_2H_3^+$ ion with respect to the cis-trans hindered rotation. Our calculation predicts that the average FH/FF distance becomes longer upon deuteron substitution of F_2H^- and $F_2H_3^+$. It is presumably due to the nature of extremely strong hydrogen bond of these species, similar to the case of $O_2H_5^+$. This should be ascribed to nuclear quantum effect (mainly zero-point effect) with respect to two FH/OH anharmonic vibrations.

Supporting Information

Figure S1 Probability density of with respect to ϕ_{HFFH} and R_{HH} obtained from (**a**) ab initio PIMD simulation of $F_2H_3^+$, (**b**) ab initio PIMD of $F_2D_3^+$, (**c**) ab initio MD of $F_2H_3^+$. (**d**) Potential energy surface with respect to ϕ_{HFFH} and R_{HH} obtained from ab initio geometry optimization calculation.

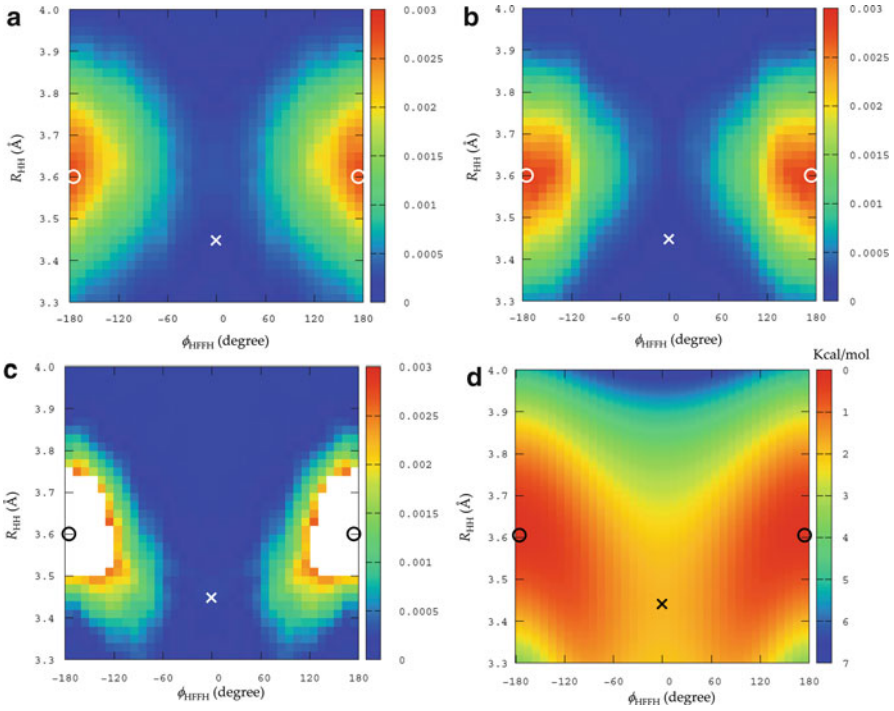

Acknowledgments We would like to thank Grant-in-Aid for Scientific Research and for the Priority Area by Ministry of Education, Culture, Sports, Science and Technology, Japan.

References

1. Steiner T (2002) Angew Chem Int Ed 41:48
2. Meot-Ner M (2005) Chem Rev 105:213
3. Marx D (2007) Chem Phys Chem 7:1848
4. Marx D, Chandra A, Tuckerman ME (2010) Chem Rev 110:2174
5. Tuckerman ME, Marx D, Klein ML, Parrinello M (1997) Science 275:817
6. Tachikawa M, Shiga M (2005) J Am Chem Soc 127:11908
7. McCoy AB, Huang X, Carter S, Landeweer MY, Bowman JM (2005) J Chem Phys 122: 1857472
8. Karpfen A, Yanoviskii O (1994) J Mol Struct (THEOCHEM) 307:81
9. Sophy KB, Kuo J-L (2009) J Chem Phys 131:224307
10. Asmis KR, Yang Y, Santambrogio G, Brümmer M, Roscioli JR, McCunn LR, Johnson MA, Kühn O (2007) Angew Chem Int Ed 46:8691

11. Ishibashi H, Hayashi A, Shiga M, Tachikawa M (2008) Chem Phys Chem 9:383
12. Yang Y, Kühn O (2011) Chem Phys Lett 505:1
13. Kawaguchi K, Hirota E (1986) J Chem Phys 84:2953
14. Hunt RD, Andrews L (1987) J Chem Phys 87:6819
15. Kawaguchi K, Hirota E (1987) J Chem Phys 87:6838
16. Kawaguchi K, Hirota E (1996) J Mol Struct 352/353:389
17. Epa C, Thorson WR (1990) J Chem Phys 93:3773
18. Del Bene JE, Jordan MJ (1999) Spectrochim Acta A 55:719
19. Swalina C, Hammes-Schiffer S (2005) J Phys Chem A 109:10410
20. Elghobashi N, González L (2006) J Chem Phys 124:174308
21. Hirata S, Yagi K, Perera SA, Yamazaki S, Hirao K (2008) J Chem Phys 128:214305
22. Hirata S, Miller EB, Ohnishi Y, Yagi K (2009) J Phys Chem A 113:12461
23. McCoy AB, Huang X, Catrter S, Bowman JM (2005) J Chem Phys 123:064317
24. Yang Y, Kühn O (2008) Z Phys Chem 222:1375
25. Suzuki K, Shiga M, Tachikawa M (2008) J Chem Phys 129:144310
26. Shiga M, Suzuki K, Tachikawa M (2010) J Chem Phys 132:114104
27. Yagi K, Hirata S, Hirao K, (2007) Theor Chem Acc 118:681
28. Benoit M, Marx D (1998) Nature 392:258
29. Marx D, Tuckerman ME, Hutter J, Parrinello M (1999) Nature 397:601
30. Tuckerman ME, Marx D, Parrinello M (2002) Nature 417:925
31. Shiga M, Tachikawa M, Miura S (2000) Chem Phys Lett 332:396
32. Hayashi A, Shiga M, Tachikawa M (2008) Chem Phys Lett 410:54
33. Koizumi A, Suzuki K, Shiga M, Tachikawa M (2011) J Chem Phys 134:031101
34. Li X-Z, Walker B, Michaelides A (2011) Proc Natl Acad Sci USA 108:6369
35. Shiga M, Tachikawa M, Miura S (2001) J Chem Phys 115:9149
36. Frisch MJ, Trucks GW, Schlegel HB et al (2004) GAUSSIAN 03, revision C.02, Gaussian Inc., Pittsburgh
37. Martyna GJ, Tuckerman ME, Klein ML (1992) J Chem Phys 97:2635
38. Martyna GJ, Tuckerman ME, Tobias DJ, Klein ML (1996) Mol Phys 87:1117
39. Tuckerman ME, Marx D, Klein ML, Parrinello M (1996) J Chem Phys 104:5579
40. Flyvbjerg H, Petersen HG (1989) J Chem Phys 91:461